Design of a REBCO thin film superconducting undulator

IOP Conf. Series: Materials Science and Engineering **101** (2015) 012053 doi:10.1088/1757-899X/101/1/012053

Design of a REBCO thin film superconducting undulator

I Kesgin[1,3], C L Doose[2], M T Kasa[2], Y Ivanyushenkov[2] and U Welp[1]

[1]Material Science Division, Argonne National Laboratory, 9700 South Cass Avenue B109, Lemont, IL 60439, USA
[2]Accelerator System Division, Argonne National Laboratory, 9700 South Cass Avenue B109, Lemont, IL 60439, USA

E-mail: ikesgin@anl.gov

Abstract. Recent developments have shown that superconducting undulators, mainly NbTi-based, outperform the existing devices. However, cooling these undulators is a challenge. REBCO (RE = rare earth, barium copper oxide) coated conductors (CCs) have been found to be a promising alternative to these materials due to their larger temperature stability margin and high engineering current densities. Here, we have investigated the feasibility of building an undulator magnetic structure using REBCO coated conductors and conducted experiments to evaluate their performance. The undulator coil has been wound with no inter-layer insulation. The critical current measurements at 77K showed that the winding of the undulator does not noticeably deteriorate the performance of the tape. Transient behaviour of the undulator has also been investigated and found to be characterized by long magnetic field decay times that result from current sharing between the windings. Steady-state operation was found to be very suitable for most undulator applications.

1. Introduction

Undulators are the heart of light sources (3rd and 4th generation) and free electron lasers (FELs) as they are the source of high–brilliance partly coherent x-ray beams. Undulators produce spatially periodically magnetic field patterns as shown in Figure 1 that interact with the charged particles. When the electrons travel in a periodic magnetic field, they experience oscillatory deflections around their average trajectory which leads to the emission of electromagnetic radiation. The wavelength of the synchrotron radiation, λ, is given by $\lambda=\lambda_u/2\gamma^2(1+K^2/2+\gamma^2\theta^2)$ where γ is the relativistic factor, θ is the polar radiation angle with respect to beam axis, λ_u is period of the magnetic pattern in the undulator, $K=0.0934\lambda_u$ [mm] B_0 [T] is the deflection parameter. Typically, high values of K are desired for achieving highly brilliant and widely tunable x-ray beams. Superconducting undulator (SCU) technology (primarily NbTi-based) has been successfully demonstrated and has surpassed the performance of the existing devices, enabling substantial increases in brilliance especially at high photon energies (i.e., > 20keV) [1]. As NbTi superconductors reach their material limitation, different materials need to be evaluated to further enhance the performance of undulators. Nb_3Sn superconductors are well-established material allowing for enhanced performance as compared to NbTi, but it requires a reaction step at high-temperature (650–700 ^oC) after the winding. Dimensional deformations of the undulator core can occur at these temperatures and the wire becomes brittle which might result in performance degradation. Recently, tremendous improvements have been made in the critical current density of REBCO (RE=rear earth, barium copper oxide) coated conductors (CCs) with

[3] To whom all correspondence should be addressed

zirconium doping [2-4]. For example, in research samples, REBCO coated conductors containing 15 mol-% Zr, a critical current density as high as 30 MA/cm^2 at 4.2 K and in a magnetic field of ~4 T perpendicular to the REBCO layer has been demonstrated [3]. This current density corresponds to an engineering current density of J_e ~ 3000 A/mm^2, a value that is substantially higher than that of NbTi (~1.43 kA/mm^2 at 3.6 T [5]), indicating that at least a factor of two increase in the on-axis field appears feasible with coated conductors compared to NbTi-based undulators. In addition, due their larger temperature margins, they can be operated at higher temperatures than NbTi which simplifies the cryogenic design. Although some attempts were made to fabricate REBCO undulators [6, 7], the behaviour of REBCO CCs in an undulator coil is still unknown. Here, we have successfully built two-period undulator magnetic structure using REBCO CCs pancake coils with opposing current directions (see Figure 1). Critical current (I_c) and field performances along with dynamic behaviour of such a magnetic structure have been evaluated at 77 K. In total, there are four pancake coils and each pancake coil is dry-wound with 55 turns.

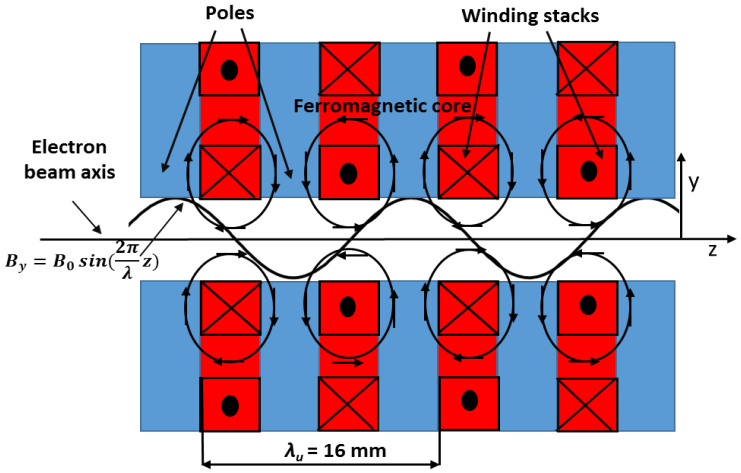

Figure 1. A sketch of an undulator showing only the major components near the electron beam.

2. Experimental

2.1. REBCO tapes

The REBCO coated conductors used in this work were fabricated by SuperPower Inc (SP). The conductor architecture consists of buffer layers of alumina, yttria, MgO and $LaMnO_3$ (LMO), deposited on 12 mm wide, non-magnetic electro-polished Hastelloy substrates followed by deposition of ~1 μm thick REBCO by metal organic chemical vapour deposition (MOCVD) [8]. Then, the tape is sliced into two 4 mm wide tapes with a U-shaped header portion. This U-slitting was implemented to have a superconducting path at the bottom of the winding stacks and further detail can be found in [9]. The superconducting film was capped by a 1-2 μm annealed Ag stabilizer and 20 μm copper electroplated on both sides totalling 40 μm.

2.2. Measurements

The electrical characterization of the resistance samples was carried out by a conventional four-contact method. The voltage drop across each lap joint was measured with a Hewlett Packard (HP) 3458A digital multi-meter (DMM) using voltage taps that spanned the entire lap joint by gradually increasing the current above the critical current of the tape and recorded. The splice resistance was then calculated by taking the value of the voltage and dividing it by the measured transport current.

Field measurements were performed with three hall probes located inside a fiberglass tube – two of the hall probes measure the component of the field in the y direction (~1 mm apart from each other) and one in x direction. This fiberglass tube is inserted in a guide tube at a distance of ~7.5 mm from

the centre of pole face of the undulator core. The hall probes can slide easily inside this guide tube. The motion is provided by a linear stage and a high-resolution encoder was used for positioning the hall probe as shown in Figure 2. The system allows for field scans along the magnet core length at a fixed current and also for field measurements versus current at a fixed location. The dynamic behaviour of the coil during fast discharging was obtained using fast data acquisition with a 24-bit Dynamic Signal Analyser (DSA) module.

2.3. Undulator winding and undulator core

The undulator magnet core was machined from a low-carbon-steel and a photo is provided in Figure 3. The width and depth of the winding grooves are 4 and 6 mm respectively. The outer connection between the double pancakes is made by a resistive double lap joint as shown in Figure 3. The pancake winding layers can also be seen in the figure. This structure has pancake coils with alternating current directions, thus creating a periodic on-axis magnetic field pattern as shown in Figure 1. For winding the core, a home-made winder was used. The tape motion and tension are provided by a stepper and two torque motors, respectively. Two tapes, the legs of the U-sliced conductor, were wound simultaneously into two neighbouring grooves. A custom-made soldering station is used to make the soldering connections on the outer windings.

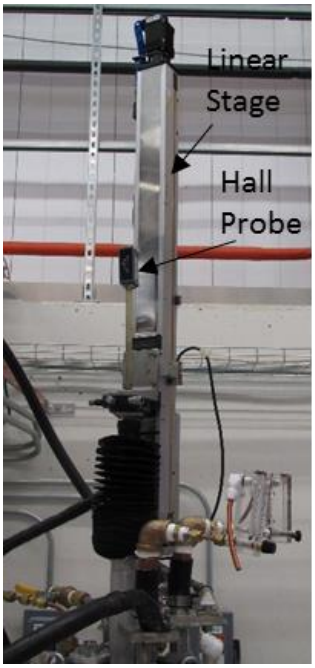

Figure 2. A photo of linear stage showing the hall probe tube connected to the stage, ready for scan.

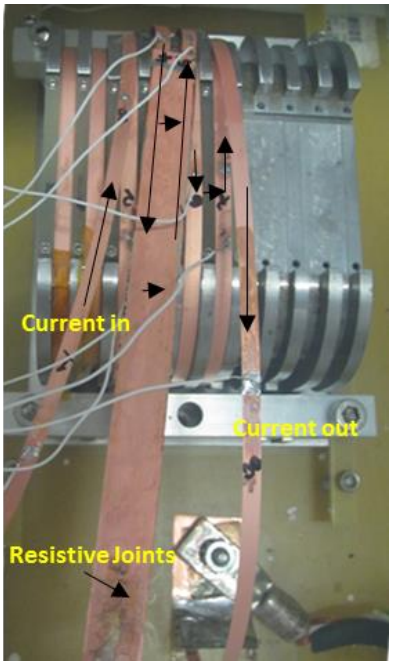

Figure 3. Undulator core with winding stacks and the current flow directions.

Electrical insulation of the windings is an important issue in the design of electromagnets. Conventional magnets wound with resistive wires cannot generate the targeted field without proper insulation because of current shorting between layers [10]; however, in superconducting DC magnets where the electrical current is ramped up and down slowly, the insulation may not be necessary. This is due to the fact that the operating current is less than the I_c of the superconducting tape and the current follows a racetrack or circular path without shorting between the layers in steady-state operation conditions due to the resistive stabilizer. Recently, this technique (no-insulation, NI) has been actively studied [11-14]. The idea was to eliminate inter-layer insulations thereby creating more compact magnet structures. The total thickness of the coated conductors used here is around 100 μm,

and a typical insulation layer might have similar thickness. Thus, eliminating the interlayer insulation effectively yields a doubling of the engineering current density. The equivalent circuit model and the difference between NI and insulation coils are highlighted in Figure 4. The figure shows an additional resistive component from the NI winding arising from eddy currents in the ferromagnetic core which is ignored in the following since the current ramp rate is low. In an insulated coil, usually R_R is very high and current flow through this path is negligible even at current values above the I_c. However, if there is no insulation, the applied-current is redistributed according to the resistance in the circuit at current values above the I_c. The total voltage across the coil obeys the following formulae when the magnet is slowly charged;

$$V_{Total} = \begin{cases} L_{Coil}\dfrac{dI_\theta}{dt} + \dfrac{V_c}{I_\theta}\left(\dfrac{I_\theta}{I_C}\right)^n = I_R R_R & I_\theta > I_C \\ L_{Coil}\dfrac{dI_\theta}{dt} & I_\theta < I_C \end{cases}, \quad (1)$$

where L_{coil}, I_{PS}, I_θ, I_R, R_θ, R_R, R_{Total} are the inductance of the coil, power supply current, current in azimuthal direction, current in the radial direction, resistance in the azimuthal direction, resistance in the radial direction and total resistance respectively.

In addition to the benefit of having a more compact system, NI winding also improves the coil protection. The specific heat and temperature margin of the HTS conductors are relatively higher than LTS conductors and *n*-values are lower. They have a slow normal zone propagation velocity (NZPV = several millimetres per second after a quench) [15]; therefore, upon a quench, the released heat remains in a relatively small hot spot inside the HTS coil for considerable times which might lead a rapid temperature increase and possibly a catastrophic failure. It was found that in NI coil, the magnet current was automatically shunted through neighbouring layers in the radial direction from its original path and the magnet is self-protected even though the operating current is higher than the magnet I_c [12, 14, 16]. Because of the aforementioned extensive benefits and also the fact that the undulator will be operated below the I_c, we chose to wind the undulator coils without inter-layer insulation (NI).

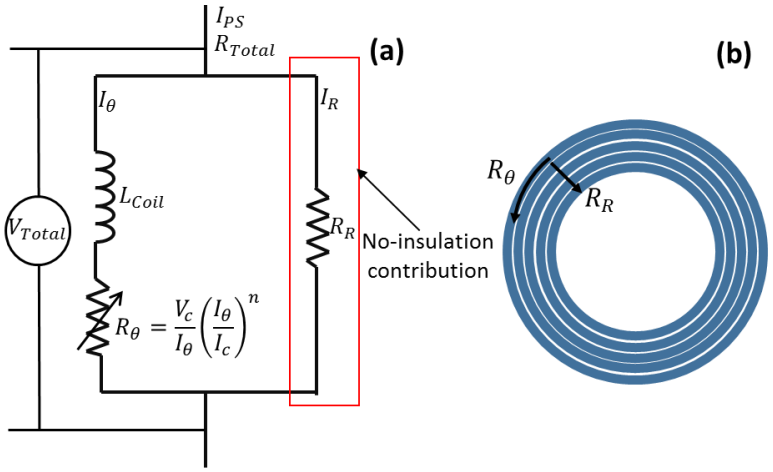

Figure 4. An equivalent circuit model for a no-insulation (NI) coil (a) and the resistances in such a coil (b).

3. Results and Discussions

The initial I_c-values of the all the tapes were almost identical (119 A). Total number of turns per pancake is 56. Figure 5 shows the I-V curve of the entire magnet. The I_c of the tape was obtained using a 1μV/cm criterion as shown in the figure with a straight horizontal line. The I_c after winding has dropped to 33.5 A indicating that only ~28 % of the I_c is retained. Due to the pronounced flux-creep at high temperatures, the I_c is effected heavily by the externally applied field [2, 17]. Very sharp decrease

in I_c with respect to applied magnetic field is typically observed up to 0.4 T at 77 K and the decrease gradually becomes less beyond the field of 0.4 T. I_c retention is found to be around 30 % at 0.52 T and 77 K in 7.5% Zr doped sample [2], having the same composition as the tape used in this study. The maximum externally applied field on the conductor is numerically calculated to be around 0.58 T. The I_c retention in the coil pack and the experimentally obtained retention reported in reference [2] almost match, implying that the tape was not noticeably damaged during the winding and cooling process.

The resistive junctions have very low resistance, R_J= 6 nΩ per one lap-joint which corresponds to resistivity value of 36 nΩ·cm^2, which is lower than the manufacturer specifications [18]. The inductance of the coil increases slightly at low current values (~5A-15A) due to the core effect and is almost constant (4 mH) up-to 36 A. The *n* value of the IV-curve has been extracted from power law fits using the maximum and minimum voltage criteria and found to be about 21 for the entire magnet. These thresholds are indicated in Figure 5 with two dashed horizontal lines.

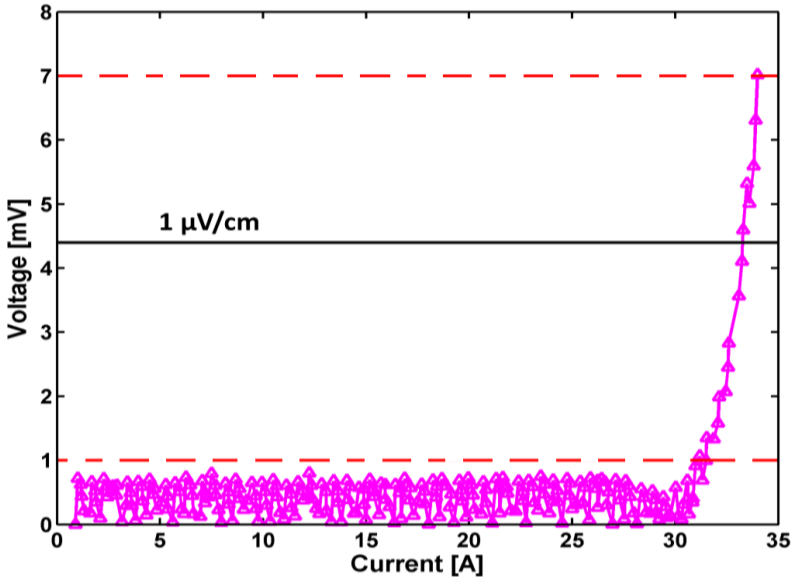

Figure 5. I-V characteristic of the undulator coil. I_c is obtained using the criterion of 1 µV/cm and the *n* value is calculated taking the maximum and minimum criteria as shown with the dashed lines.

Magnetic field scans are performed at different current values at a distance of 7.4 mm from the magnet core along the beam axis (see Figure 1 for location of the beam axis) and shown in Figure 6. We measured only one partial magnetic structure with four pancake coil windings. These pancake coils are connected with resistive joints on the outside and through the header section of the U-slit tapes inside of the winding pack. Field scans show five magnetic peaks that correspond to the poles of the magnetic core. The generated magnetic field is stable (no fluctuations are observed in the scans). A non-symmetric field component at lower magnetic fields can be seen in the figure. This is due to the non-symmetric winding of the core. In other words, the length of the ferromagnetic core on one side is longer than on the other side which results in non-symmetric field profiles along the z direction at a distance of 7.4 mm in the y direction. Field versus current measurements were also performed and are displayed in Figure 7. These data was taken from Figure 6 at a distance of 7.4 cm from the left edge of the undulator magnet core. Up to the I_c of the coil, the magnetic field versus current curve is perfectly linear (R^2=1); however, it approaches saturation at currents beyond I_c. This deviation from the linear B vs. I curve at $I > I_c$ is caused by current sharing and shorting between the winding layers.

To understand the dynamic or transient behaviour of the undulator coil, sudden discharge tests were performed. Before the electrical measurement, the coil was in the steady-state (below I_c) and then the current was cut off suddenly as shown in Figure 8. In the figure, the left y-axis is related to the

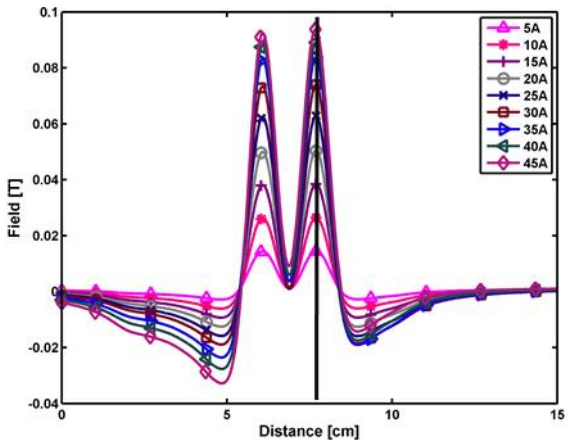

Figure 6. Magnetic field scans at a distance of 7.4 mm from the magnet pole along the z direction at different currents.

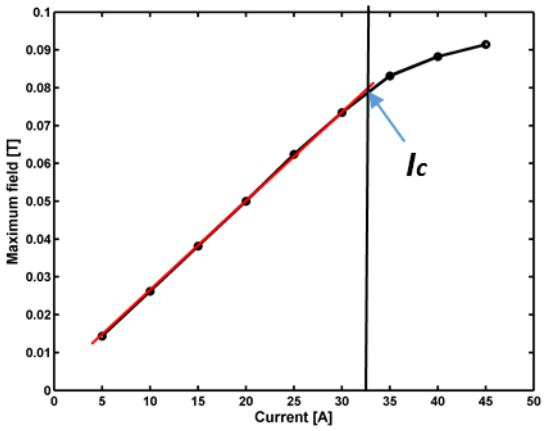

Figure 7. Field versus curent that was obtained form the straight line at 7.5 cm in Figure 6. Beyond I_c, the field approaches saturation.

normalized field and current. The right y-axis is related to the normalized voltage on the coil pack. The decay of the current externally supplied to the coil is considerably faster than the magnetic field decay. It can be seen from the figure, although it takes few milliseconds for current to decay (time constant, τ=2.88 ms), the decay time for the magnetic field and the voltage take considerably longer (τ=0.7 s). This is due to the current sharing between the layers, which enables current to keep circulating on closed trajectories and maintaining the magnetic flux according to Lenz's law. There is also a contribution of the eddy current in the ferromagnetic core to the signal at some degree as the core and coil packs are inductively coupled. Complete relaxation of all three variables takes about 10 seconds. Such behaviour is highly undesired in devices where fast switching of the current is required for example for fast switching of the polarization of the x-ray beam.

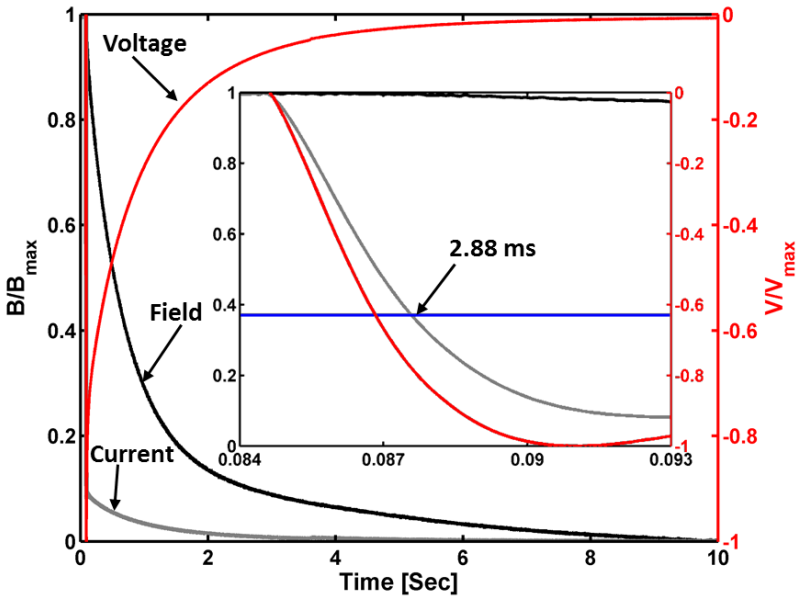

Figure 8. Sudden discharging test from 28 A steady-state operation showing voltage (across the undulator coil), current and field profiles. Inset shows magnified initial current decay portion of the overall performance.

4. Conclusions

We have investigated the feasibility of using REBCO coated conductors in planar undulator applications and shown that an undulator magnetic structure can actually be built using RECO coated conductors with no significant degradation in the performance of the REBCO CCs. The performance of the undulator has been evaluated at 77 K. The I_c retention has been found to be reasonable after the undulator core winding indicating that the undulator winding and cooling cycles do not deteriorate the performance of the undulator significantly. The dynamic behaviour of the undulator core is characterized by long time constants of the field decay which result from current sharing in the NI windings and which poses limits in switching applications. However, steady-state mode performances have been found to be suitable for most of the undulator applications. The generated field is very stable and desired magnetic field can be obtained with no fluctuation. This would suggest that NI windings are perfect for most of undulators.

5. Acknowledgments

This work was supported by the U.S. Department of Energy, Office of Science, Materials Sciences and Engineering Division. The authors would like to thank Yifei Zhang from SuperPower Inc. for useful discussions and Kurt Boerste form magnetic devices group at Argonne National Laboratory for technical help.

6. References

[1] Ivanyushenkov Y, Doose C, Fuerst J, Hasse Q, Kasa M and Shiroyanagi Y 2014 Test Results of a Planar Superconducting Undulator for the Advanced Photon Source *IEEE Trans. Appl. Supercond.* **24** 1-4

[2] Selvamanickam V, *et al.* 2010 Enhanced and uniform in-field performance in long (Gd, Y)-Ba-Cu-O tapes with zirconium doping fabricated by metal-organic chemical vapor deposition *Supercond. Sci. Technol.* **23** 014014-20

[3] Xu A, Delgado L, Khatri N, Liu Y, Selvamanickam V, Abraimov D, Jaroszynski J, Kametani F and Larbalestier D C 2014 Strongly enhanced vortex pinning from 4 to 77 K in magnetic fields up to 31 T in 15 mol.% Zr-added (Gd, Y)-Ba-Cu-O superconducting tapes *APL Materials* **2** 046111

[4] Selvamanickam V, Gharahcheshmeh M H, Xu A, Galstyan E, Delgado L and Cantoni C 2015 High critical currents in heavily doped (Gd,Y)$Ba_2Cu_3O_x$ superconductor tapes *Appl. Phys. Lett.* **106** 032601

[5] Kim S H, Doose C, Kustom R L, Moog E R and Vasserman I 2005 R&D of Short-Period NBTI and Nb_3Sn Superconducting Undulators for the APS *Proceedings of PAC* 2419-21

[6] Boffo C and Gerhard T 2013 High-temperature superconductor magnet system, patent # WO/2012/013205 (Germany), 8,849,364 (US)

[7] Prestemon S, Arbelaez D, Davies S, Dietderich D R, Lee D, Minervini F and Schlueter R D 2011 Development and Analysis of HTS-Undulator Components for FEL Applications *IEEE Trans. Appl. Supercond.* **21** 1880-3

[8] Selvamanickam V, *et al.* 2009 High Performance 2G Wires: From R&D to Pilot-Scale Manufacturing *IEEE Trans. Appl. Supercond.* **19** 3225-30

[9] Kesgin I, Kasa M, Doose L C, Ivanyushenkov Y and Welp U 2015 Feasibility and electromagnetic analysis of a REBCO superconducting undulator *to be submitted*

[10] Sukjin C, Hyun Chul J, Young Jin H, Seungyong H and Tae Kuk K 2012 A Study on the No Insulation Winding Method of the HTS Coil *IEEE Trans. Appl. Supercond.* **22** 4904004

[11] Seungyong H, Dong Keun P, Voccio J, Bascunan J and Iwasa Y 2012 No-Insulation (NI) HTS Inserts for >1 GHz LTS/HTS NMR Magnets *IEEE Trans. Appl. Supercond.* **22** 4302405

[12] Young-Gyun K, Seungyong H, Kwang Lok K, Oh Jun K and Haigun L 2012 Investigation of HTS Racetrack Coil Without Turn-to-Turn Insulation for Superconducting Rotating Machines *IEEE Trans. Appl. Supercond.* **22** 5200604

[13] Choi Y H, Hahn S, Song J B, Yang D G and Lee H G 2011 Partial insulation of GdBCO single pancake coils for protection-free HTS power applications *Supercond. Sci. Technol.* **24** 125013
[14] Seungyong H, Dong Keun P, Bascunan J and Iwasa Y 2011 HTS Pancake Coils Without Turn-to-Turn Insulation *IEEE Trans. Appl. Supercond.* **21** 1592-5
[15] Kim S B, Saito A, Kaneko T, Joo J H, Jo J M, Han Y J and Jeong H S 2012 The Characteristics of the Normal-Zone Propagation of the HTS Coils With Inserted Cu Tape Instead of Electrical Insulation *IEEE Trans. Appl. Supercond.* **22** 4701504-
[16] Xudong W, Seungyong H, Youngjae K, Juan B, John V, Haigun L and Yukikazu I 2013 Turn-to-turn contact characteristics for an equivalent circuit model of no-insulation ReBCO pancake coil *Supercond. Sci. Technol.***26** 035012
[17] Selvamanickam V, Chen Y, Xie J, Zhang Y, Guevara A, Kesgin I, Majkic G and Martchevsky M 2009 Influence of Zr and Ce doping on electromagnetic properties of (Gd,Y)-Ba-Cu-O superconducting tapes fabricated by metal organic chemical vapor deposition *Physica C* **469** 2037-43
[18] SuperPower® 2G HTS Wire Specifications Available online: http://www.superpower-inc.com/system/files/SP_2G+Wire+Spec+Sheet_for+web_0509.pdf